

## Influence of structural system measures on the dynamic characteristics of a multi-span cable-stayed bridge

Fangfang Geng<sup>1a</sup>, Youliang Ding<sup>\*1</sup>, Hongen Xie<sup>1b</sup>, Jianyong Song<sup>2c</sup>  
and Wanheng Li<sup>2d</sup>

<sup>1</sup>Key Laboratory of Concrete and Prestressed Concrete Structures of Ministry of Education,  
Southeast University, Nanjing 210096, China

<sup>2</sup>Research Institute of Highway Ministry of Transport, Beijing 100088, China

(Received November 7, 2012, Revised May 12, 2014, Accepted June 20, 2014)

**Abstract.** A three-dimensional finite element model for the Jiashao Bridge, the longest multi-span cable-stayed bridge in the world, is established using the commercial software package ANSYS. Dynamic characteristics of the bridge are analyzed and the effects of structural system measures including the rigid hinge, auxiliary piers and longitudinal constraints between the girders and side towers on the dynamic properties including modal frequency, mode shape and effective mass are studied by referring to the Jiashao Bridge. The analysis results reveal that: (i) the installation of the rigid hinge significantly reduces the modal frequency of the first symmetric lateral bending mode of bridge deck. Moreover, the rigid hinge significantly changes the mode shape and effective mass of the first symmetric torsional mode of bridge deck; (ii) the layout of the auxiliary piers in the side-spans has a limited effect on changing the modal frequencies, mode shapes and effective masses of global vibration modes; (iii) the employment of the longitudinal constraints significantly increases the modal frequencies of the vertical bending modes and lateral bending modes of bridge deck and have significant effects on changing the mode shapes of vertical bending modes and lateral bending modes of bridge deck. Moreover, the effective mass of the first anti-symmetric vertical bending of bridge deck in the longitudinal direction of the fully floating system is significantly larger than that of the partially constrained system and fully constrained system. The results obtained indicate that the structural system measures of the multi-span cable-stayed bridge have a great effect on the dynamic properties, which deserves special attention for seismic design and wind-resistant design of the multi-span cable-stayed bridge.

**Keywords:** multi-span cable-stayed bridge; dynamic characteristics; rigid hinge; longitudinal constraint; auxiliary pier

### 1. Introduction

The contemporary cable-stayed bridge is becoming more and more popular and being used where previously a suspension bridge might have been chosen. The increasing attention on cable-

---

\*Corresponding author, Professor, E-mail: [civilding@163.com](mailto:civilding@163.com)

<sup>a</sup>Ph.D. Student, E-mail: [gengfangfang\\_1983@163.com](mailto:gengfangfang_1983@163.com)

<sup>b</sup>Master, E-mail: [528949073@qq.com](mailto:528949073@qq.com)

<sup>c</sup>Ph.D., E-mail: [623151019@qq.com](mailto:623151019@qq.com)

stayed bridges is not only due to their inherent beauty but also to the efficient utilization of structural materials and the increased stiffness over suspension bridges. For long-span cable-stayed bridges, the multi-span cable-stayed bridges with three or more towers have been a recent design trend (Virlogeux 1999; Ni *et al.* 2005). Typical examples of this bridge type are the Millau Viaduct Bridge in France, the Maracaibo Bridge in Venezuela, the Rion-Antirion Bridge in Greece, the Mezcala Bridge in Mexico, the Dongting Lake Bridge in China, and the Ting Kau Bridge in Hong Kong (Virlogeux 1999; Barre *et al.* 1999; Papanikolas 2003; Ni *et al.* 2005). The longest multi-span cable-stayed bridge in the world is Jiashao Bridge in China, which is a six-tower cable-stayed bridge with the total length 2680 m.

Compared with a conventional three-span cable-stayed bridge with two towers, there are two major problems in the design of multi-span cable-stayed bridges. One is the insufficient system stiffness arose from the central tower(s). In the conventional cable-stayed bridges with two towers, each of the towers is connected through outermost stay cables to the fixed anchorage or anchor pier, which can provide effective support to the towers (Ni *et al.* 2005). However, in a multi-span cable-stayed bridge, the beneficial effect of the fixed anchorage or anchor pier diminishes for the central tower(s). Hence, the structural responses of a multi-span cable-stayed bridge such as deflections of main girders and internal forces at the bottom of towers are increased significantly under unbalanced live loadings compared with a conventional cable-stayed bridge. The commonly used structural measures to increase the system stiffness includes three aspects: i) stiff central tower(s) such as the Millau Viaduct Bridge in France and the Rion-Antirion Bridge in Greece (Barre *et al.* 1999; Papanikolas 2003); ii) stabilizing cables in the longitudinal direction to connect the top of the central tower(s) to the deck near the side towers such as the Ting Kau Bridge in Hong Kong (Ni *et al.* 2005); iii) auxiliary piers additionally installed in each side span such as the Mezcala Bridge in Mexico and the Sepoong Bridge in Korea (Virlogeux 1999). Another important problem in the design of multi-span cable-stayed bridges is the large temperature deformation in the long girders. For bridge girders and stay cables, large temperature deformation will affect the safety and serviceability. Meanwhile, large temperature deformation will increase the internal forces at the bottom of side towers. The commonly used structural measures to reduce the temperature effects includes two aspects: i) longitudinal constraints between the girders and side towers such as the Millau Viaduct Bridge in France and the Jiashao Bridge in China; ii) rigid hinge to release the temperature-induced deformation in the girders such as the Jiashao Bridge in China.

The aforementioned structural measures mainly improve the static performance of multi-span bridges under live loadings and temperature action. It is necessary to investigate the influences of these structural measures on the structural dynamic performance under the earthquake and wind actions. Ni *et al.* (2005) investigated the dynamic properties of multi-span cable-stayed bridges with stabilizing cables and the effect of stabilizing cables on bridge seismic responses by referring to the Ting Kau Bridge. The analysis results reveal that the longitudinal stabilizing cables bring about a number of global modes with strong modal interaction among the deck, towers, and cables. As a whole, the stabilizing cables are favorable in the reduction of seismic responses of the bridge. Su *et al.* (2003) investigated the wind-induced buffeting responses of the Ting Kau Bridge in the time domain for various mean wind velocities, taking into consideration both geometric nonlinearity and aeroelastic effects. The aerodynamic behavior of the multi-span cable-stayed bridge can then be obtained and the safety performance of the bridge against strong wind can further be evaluated. Li *et al.* (2009) investigated the seismic behaviors of a three-tower cable-stayed bridge with different longitudinal constraints between bridge girders and towers. Three structural systems including Rigid System (RS), Floating System (FS) and Passive Energy

Dissipation System (PEDS) were studied and failure modes of the three different systems were further concluded. However, compared with the research efforts devoted to dynamic responses of conventional three-span cable-stayed bridges (Zhang *et al.* 2001; Ren *et al.* 2005; Li *et al.* 2007; Ren *et al.* 2007; Ding *et al.* 2008; Li *et al.* 2010; Raheem *et al.* 2011), only a few works have been focused on the dynamic performance of multi-span cable-stayed bridges. Considering the structural dynamic characteristics including modal frequencies and mode shapes form the basis of earthquake and wind resistance analysis of multi-span cable-stayed bridges, it is especially desirable to understand the effects of the aforementioned structural measures on the dynamic characteristics of multi-span cable-stayed bridges.

Based on the aforementioned motivation, by taking the Jiashao Bridge as a paradigm, the influences of structural system measures including the rigid hinge, auxiliary piers and longitudinal constraints between the girders and towers on the dynamic properties of the multi-span cable-stayed bridge are studied in this article. A three-dimensional finite element model of the Jiashao Bridge is developed using the nonlinear finite element software ANAYS. Modal analysis is conducted to obtain the dynamic characteristics including the modal frequencies and mode shapes of lateral, vertical, torsional and longitudinal vibrations of the bridge, on the basis of which the effects of important structural measures on the dynamic characteristics of this type of bridge are discussed in detail to give an insight into some unique features. The obtained results can provide valuable references for earthquake and wind resistance design of multi-span cable-stayed bridges.

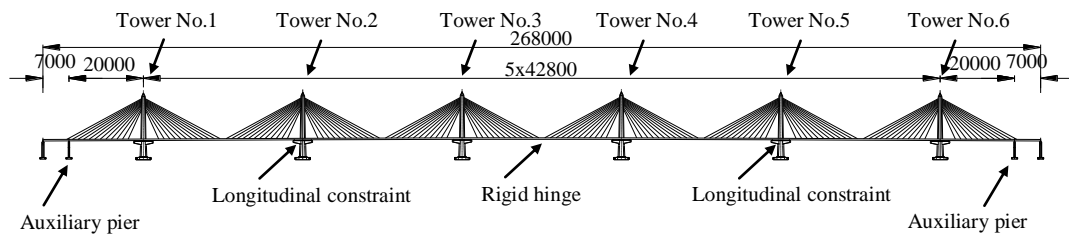
## 2. Bridge description

The subject of this study is Jiashao Bridge shown in Fig. 1(a), which is a six-tower cable-stayed bridge that crosses the Hangzhou Bay, along the highway between Jiaxing and Shaoxing in China. The total length of the bridge is 2680m with the span arrangement of 70 m+200 m+5×428 m+200 m+70 m, which is the longest multi-span cable-stayed bridge in the world. Fig. 1(b) shows the schematic elevation view of the Jiashao Bridge. Its six single-leg towers are 172.174 m high supporting the bridge deck in conjunction with stay cables. There are 288 main stay cables in four planes anchored to the deck edge girders at 15 m intervals. The bridge deck is separated into two carriageways and each carriageway is an aerodynamically shaped closed steel box girder with 24 m wide and 4 m high. The two steel box girders are connected by the cross-beam at 30m intervals. Fig. 1(c) shows the typical deck cross-section of the bridge.

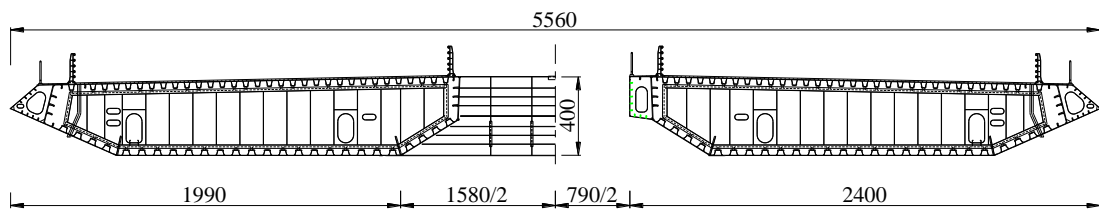
In order to overcome the problems of insufficient system stiffness and large temperature deformation in the long girders, three important structural measures are applied in the design of Jiashao Bridge as shown in Fig. 1(b): (i) A rigid hinge is employed in the middle of the main girder; (ii) In each side span, one auxiliary pier is additionally installed besides the end pier; (iii) The longitudinal constraints between the girders and side tower No. 2, the girders and side tower No. 5 are employed, respectively. Among three structural measures, the rigid hinge is the key measure to solve the problem of temperature action on the long girders. The “drawer-type” rigid hinge is employed in the design as shown in Fig. 2. The design objective of the rigid hinge is to meet the requirements of loading capacity under normal traffic conditions. Moreover, the lateral displacement, vertical displacement and the rotation around the longitudinal axis between the two ends of the main girder adjacent to the rigid hinge are coupled and the longitudinal displacement constraint between the two ends is released, which can automatically adapt to changes in longitudinal deformation due to ambient temperature variations.



(a) View of Jiashao Bridge



(b) Elevation of Jiashao Bridge (unit: cm)



(c) Cross section of bridge deck (unit: cm)

Fig. 1 Jiashao Bridge

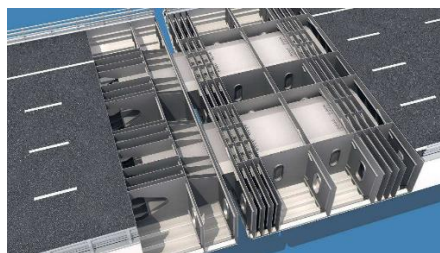


Fig. 2 “drawer-type” rigid hinge

### 3. Finite element model of the bridge

#### 3.1 Finite element model

A three-dimensional finite element model of the Jiashao Bridge has been developed by use of

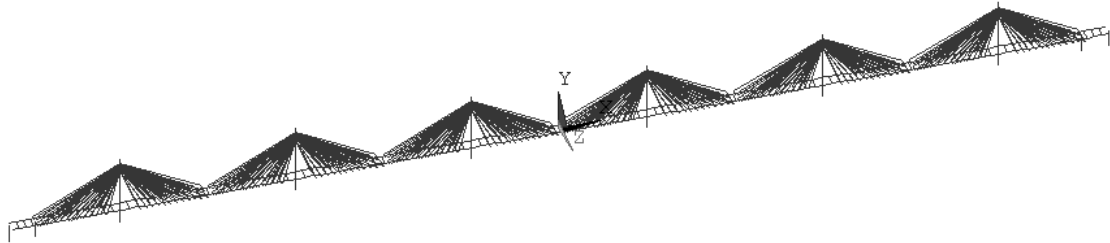


Fig. 3 Finite element model of Jiashao Bridge

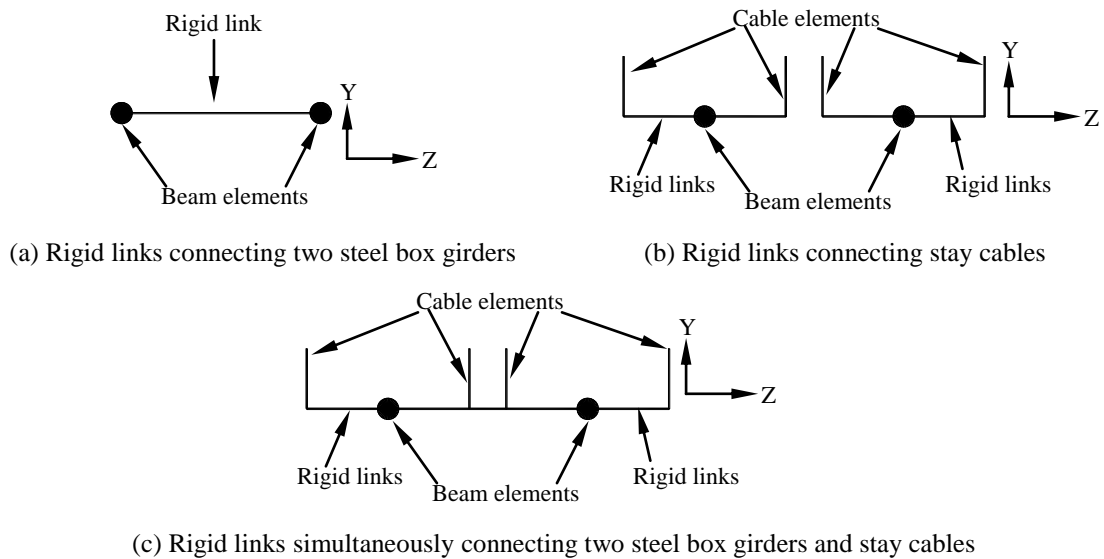
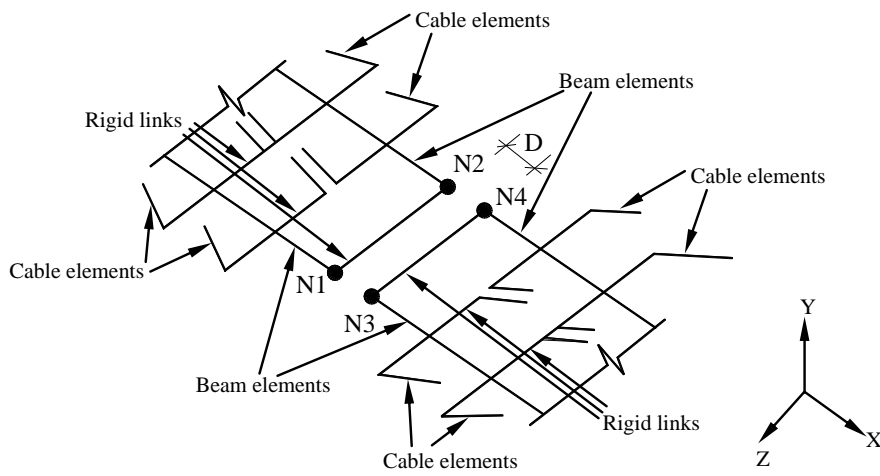


Fig. 4 Detailed finite element modeling for rigid links

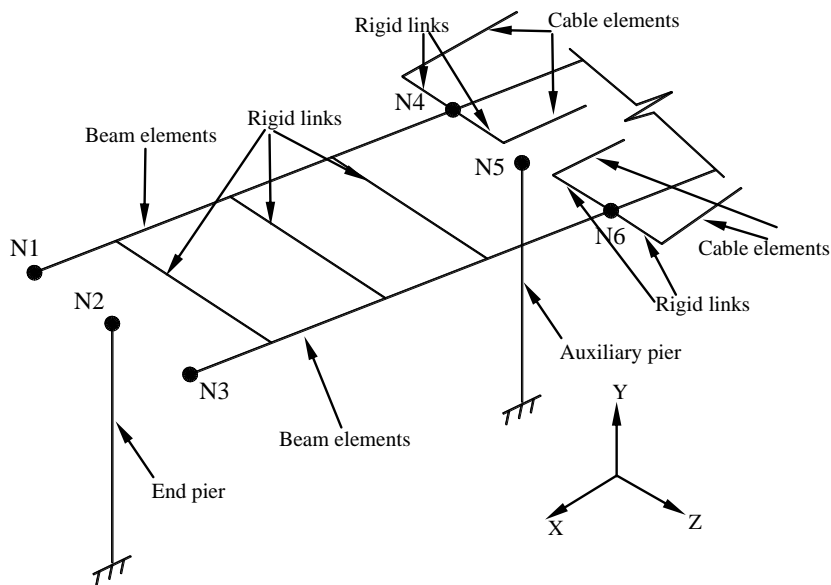
the commercial software package ANSYS. The finite element model involves 1402 nodes and 1872 elements, as shown in Fig. 3. In this model, a double-girder model is used to simulate the bridge deck system when conducting dynamic analysis. The two steel box girders are modeled as Timoshenko's beam elements with 6 degrees of freedom (DOFs) at each node, which account for transverse shear deformation, biaxial bending and axial strain (Wang *et al.* 2010). And the cross-beams connecting two steel box girders are modeled as rigid links at 30m intervals as shown in Fig. 4(a). The bridge towers and piers are also modeled as Timoshenko's beam elements. A 2-node truss element is used to simulate the stay cables, which accounts for only tension and no compression based on the real condition. Considering the geometric stiffness of stay cables under dead loading, the Ernst equivalent elastic modulus for stay cables is adopted (Ni *et al.* 2005). Rigid links at 15m intervals are used to connect the cables in four planes to the girders as shown in Fig. 4(b). Fig. 4(c) further shows the case of rigid links simultaneously connecting two steel box girders and four stay cables.

The detailed finite element modeling for three important structural measures are described as follows:

(i) Modeling of the rigid hinge in the middle of the main girder: As shown in Fig. 5(a), constraints are applied to restrict the motion of bridge deck to allow only longitudinal displacement  $X$  between the two ends of the girders adjacent to the rigid hinge. The length  $D$  of the gap between the two ends of the girders is 1.0m according to the design drawings. Thus, the constraint equations of DOFs (including  $UX$ ,  $UY$ ,  $UZ$ ,  $ROTX$ ,  $ROTY$  and  $ROTZ$ ) for the nodes  $N1 \sim N4$  shown in Fig. 5(a) can be defined as:  $UY(N1)=UY(N3)$ ,  $UY(N2)=UY(N4)$ ,  $UZ(N1)=UZ(N3)$ ,  $UZ(N2)=UZ(N4)$ ,  $ROTX(N1)=ROTX(N3)$ ,  $ROTX(N2)=ROTX(N4)$ ,  $ROTY(N1)=ROTY(N2)$ ,  $ROTY(N2)=ROTY(N4)$ ,  $ROTZ(N1)=ROTZ(N3)$ ,  $ROTZ(N2)=ROTZ(N4)$ .

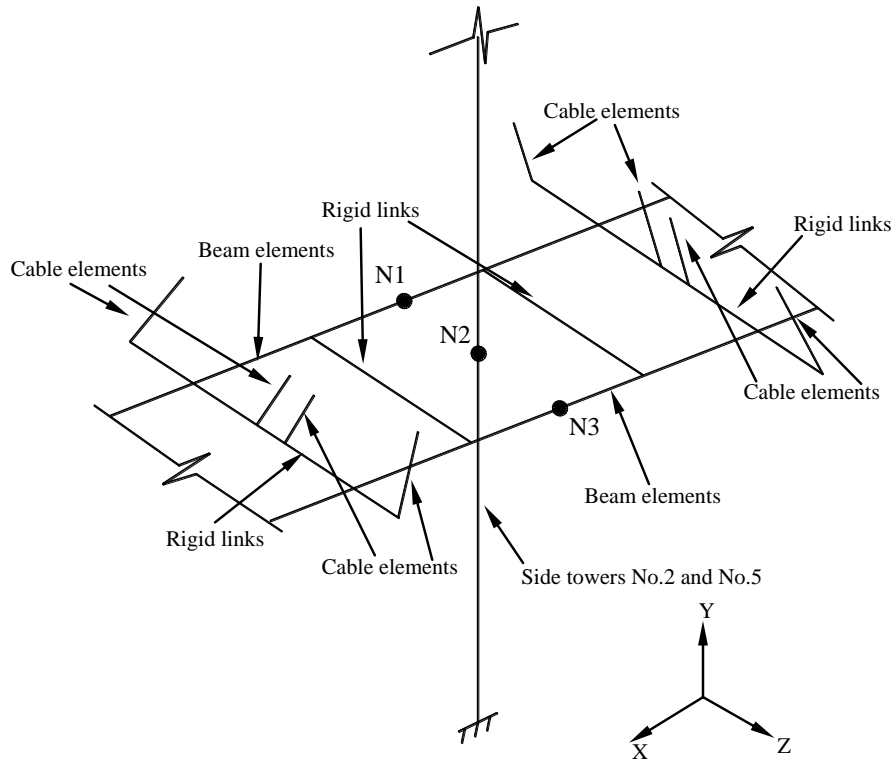


(a) Rigid hinge in the middle of the main girder



(b) Auxiliary pier and end pier in each side span

Fig. 5 Detailed finite element modeling for key measures



(c) Longitudinal constraints between the girders and side towers No.2 and No.5

Fig. 5 Continued

(ii) Modeling of auxiliary pier in each side span: As shown in Fig. 5(b), constraints are applied to restrict the motion of bridge deck at all bridge piers including auxiliary pier and end pier to allow only longitudinal displacement X and rotations about the Y and Z axes. Thus, the constraint equations of DOFs for the nodes N1 ~ N6 shown in Fig. 5(b) can be defined as:  $UY(N1)=UY(N2)=UY(N3)$ ,  $UY(N4)=UY(N5)=UY(N6)$ ,  $UZ(N1)=UZ(N2)=UZ(N3)$ ,  $UZ(N4)=UZ(N5)=UZ(N6)$ ,  $ROTX(N1)=ROTX(N2)=ROTX(N3)$ ,  $ROTX(N4)=ROTX(N5)=ROTX(N6)$ .

(iii) Modeling of longitudinal constraints between the girders and side towers No.2 and No.5: As shown in Fig. 5(c), constraints are applied to restrict the deck from moving in the longitudinal, lateral and vertical directions at bridge towers No. 2 and No. 5. Thus, the constraint equations of DOFs for the nodes N1~N3 shown in Fig. 5(c) can be defined as:  $UX(N1)=UX(N2)=UX(N3)$ ,  $UY(N1)=UY(N2)=UY(N3)$ ,  $UZ(N1)=UZ(N2)=UZ(N3)$ . It should be noted that for other towers No.1, No.3, No.4 and No.6, constraints are applied to restrict the deck from moving in the lateral and vertical directions. Thus, the constraint equations of DOFs for the nodes N1 ~ N3 can be defined as:  $UY(N1)=UY(N2)=UY(N3)$ ,  $UZ(N1)=UZ(N2)=UZ(N3)$ .

### 3.2 Dynamic properties of the bridge

The modal analysis of the Jiashao Bridge is conducted with the developed finite element

model. The static equilibrium state of the bridge, which is the initial configuration for modal analysis, is achieved by geometrically nonlinear analysis of the bridge under dead loadings (Ni *et al.* 2005, He *et al.* 2009). The LANCZOS eigenvalue solver is adopted for modal analysis. Main vibration modes of finite element model are listed in Table 1 and part of them is shown in Fig. 6. Table 2 further illustrates the effective mass and modal participation factor for each global vibration mode for different directions except local vibration modes No.16~19. In Table 2, the calculated effective mass and modal participation factor shown in bold style indicate the dominating vibration modes affecting global dynamic responses for different directions. It should be noted that in the modal analysis using the software package ANSYS the extraction number of vibration modes is 100.

The modal analysis results reveal the following dynamic characteristics of the bridge:

(i) The longitudinal floating vibration mode doesn't occur due to the longitudinal constraints between the bridge girders and two bridge towers. From Table 2, it can be seen that the anti-symmetric vertical bending modes of bridge deck including modes No. 2 and No. 10 have relative large contributions to the longitudinal dynamic responses of the bridge.

(ii) The first natural frequency of the bridge is 0.2274 Hz, which corresponds to the first symmetric vertical bending of bridge deck. And the natural frequency of the second symmetric vertical bending mode of bridge deck is 0.3085 Hz. From Table 2, it can be seen that the symmetric vertical bending modes of bridge deck including modes No. 1 and No. 9 mainly dominate the vertical dynamic responses of the bridge in comparison with the anti-symmetric vertical bending modes of bridge deck.

Table 1 Vibration modes of finite element model of Jiashao Bridge

Mode No.	Modal frequency /Hz	Description
1	0.2274	1st symmetric vertical bending of bridge deck + symmetric longitudinal bending of bridge tower
2	0.2615	1st anti-symmetric vertical bending of bridge deck + anti-symmetric longitudinal bending of bridge tower
3	0.2894	1st symmetric lateral bending of bridge tower
4	0.2907	1st anti-symmetric lateral bending of bridge tower
5	0.2928	2nd symmetric lateral bending of bridge tower
6	0.2950	2nd anti-symmetric lateral bending of bridge tower
7	0.2965	3rd symmetric lateral bending of bridge tower
8	0.2970	3rd anti-symmetric lateral bending of bridge tower
9	0.3085	2nd symmetric vertical bending of bridge deck + symmetric longitudinal bending of bridge tower
10	0.3618	2nd anti-symmetric vertical bending of bridge deck + anti-symmetric longitudinal bending of bridge tower
16~19	0.6779	Longitudinal bending of bridge piers
21	0.7087	1st symmetric lateral bending of bridge deck + symmetric lateral bending of bridge tower
33	0.8956	1st anti-symmetric lateral bending of bridge deck + anti-symmetric lateral bending of bridge tower
43	1.1361	1st symmetric torsion of bridge deck
44	1.1389	2nd symmetric torsion of bridge deck
45	1.1391	3rd symmetric torsion of bridge deck

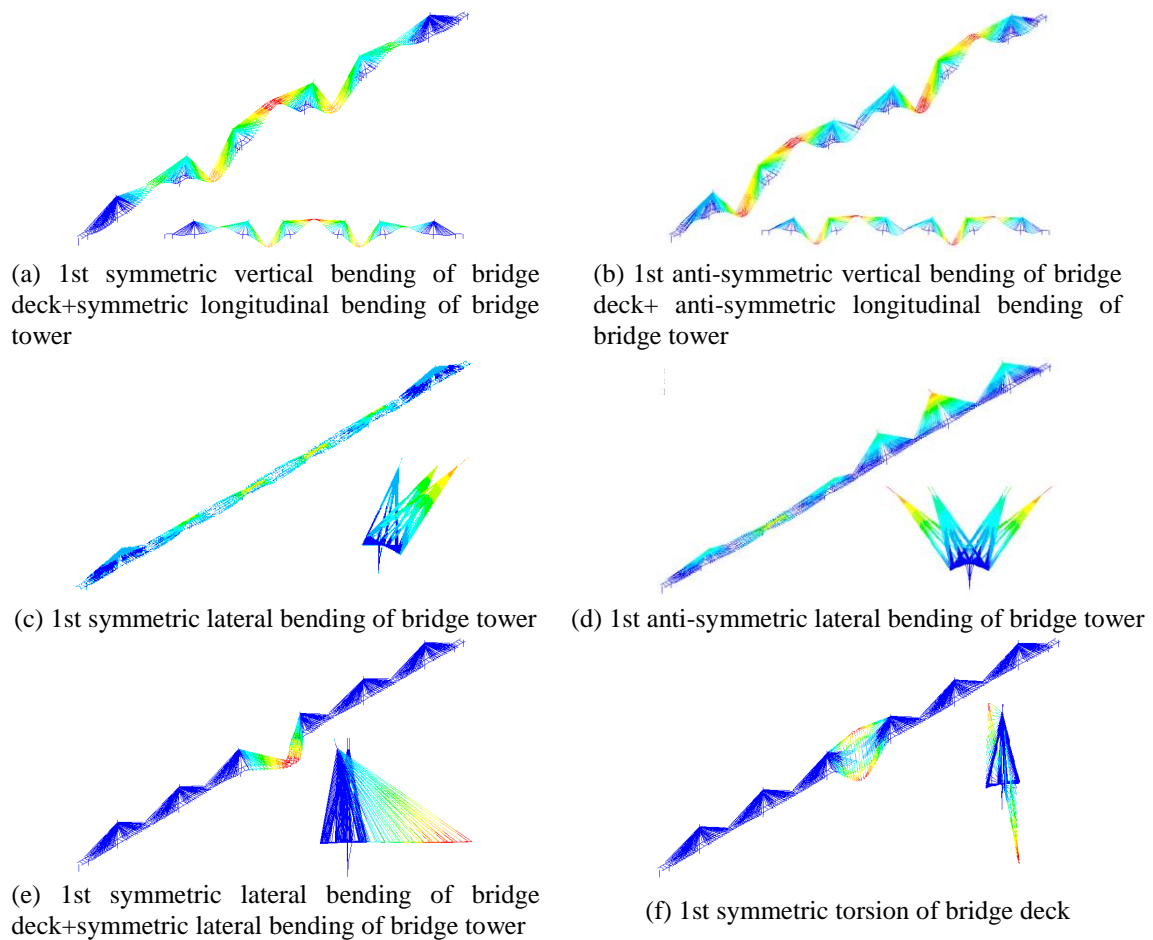


Fig. 6 Mode shapes of the bridge

(iii) The natural frequency of the first symmetric lateral bending of bridge tower is found to be 0.2894Hz, which is the third global vibration mode. Hence, the bridge towers are flexible with regard to the lateral bending. From Table 2, it can be seen that the symmetric lateral bending modes of bridge tower and bridge deck including modes No. 3, No. 5, No. 7 and No. 21 mainly dominate the transverse dynamic responses of the bridge in comparison with the anti-symmetric lateral bending modes of bridge tower and bridge deck.

(iv) The 16th to the 19th modes are longitudinal local bending of bridge piers with the same frequency of 0.6779Hz. Because there are no longitudinal displacement constraints between the girders and piers, the vibration features of the bridge piers in the longitudinal direction are similar to the cantilever beams;

(v) The first lateral bending mode of the bridge deck with a frequency of 0.7087Hz occurs at the 21st global mode, which is higher than the corresponding value 0.2274Hz of the first vertical bending mode. Thus, the in-plane stiffness of bridge deck is weaker than the out-plane stiffness;

(vi) The first torsional mode of the bridge deck with a frequency of 1.1361Hz occurs at the 43rd global mode, which is higher than the corresponding value 0.224Hz of Ting Kau Bridge (a

Table 2 Effective mass and modal participation factor for each global vibration mode

Mode No.	X direction (Longitudinal direction)		Y direction (Vertical direction)		Z direction (Transverse direction)	
	Effective mass	Participation factor	Effective mass	Participation factor	Effective mass	Participation factor
1	-8.720E-01	7.603E-01	<b>2.974E+02</b>	<b>8.845E+04</b>	-2.640E-06	6.990E-12
2	<b>-1.247E+03</b>	<b>1.560E+06</b>	8.180E-02	6.690E-03	-1.130E-05	1.270E-10
3	-7.300E-07	5.330E-13	1.840E-06	3.370E-12	<b>9.857E+03</b>	<b>9.720E+07</b>
4	-5.560E-07	3.090E-13	-1.720E-06	2.970E-12	5.610E-02	3.140E-03
5	-7.380E-07	5.440E-13	1.230E-06	1.520E-12	<b>3.395E+03</b>	<b>1.150E+07</b>
6	-1.070E-06	1.140E-12	8.550E-07	7.320E-13	-4.490E-02	2.020E-03
7	1.390E-07	1.930E-14	5.510E-07	3.040E-13	<b>2.870E+03</b>	<b>8.240E+06</b>
8	6.610E-08	4.370E-15	4.360E-07	1.900E-13	3.800E-02	1.440E-03
9	4.020E-01	1.616E-01	<b>-1.017E+03</b>	<b>1.030E+06</b>	9.300E-06	8.650E-11
10	<b>9.717E+02</b>	<b>9.442E+05</b>	-7.720E-02	5.960E-03	-2.170E-06	4.710E-12
21	3.870E-07	1.490E-13	2.520E-08	6.350E-16	<b>3.285E+03</b>	<b>1.080E+07</b>
33	-8.920E-08	7.960E-15	-4.050E-06	1.640E-11	1.675E-01	2.810E-02
43	1.090E-06	1.180E-12	-5.230E-07	2.740E-13	<b>-5.328E+02</b>	<b>2.838E+05</b>
44	-2.130E-05	4.530E-10	2.190E-06	4.800E-12	2.170E-03	4.710E-06
45	-2.710E-06	7.370E-12	-1.990E-06	3.950E-12	<b>-9.264E+01</b>	<b>8.583E+03</b>

three-tower cable-stayed bridge). Thus, the higher torsional stiffness of the bridge deck is favorable for wind-resistance performance. From Table 2, it can be seen that the first and third torsional modes of the bridge deck (modes No. 43 and No. 45) have relative large contribution to the transverse dynamic responses of the bridge.

#### 4. Influence of rigid hinge on the dynamic characteristics

As mentioned in Section 2, the rigid hinge in the middle of the main girder is very important to release the temperature-induced deformation in the girder. In this section, the effect of rigid hinge on the dynamic characteristics of the bridge is investigated. The contrast analytical model without rigid hinge is developed and the modal analysis result of the contrast model is shown in Table 3. Mode shapes of the contrast model without rigid hinge are shown in Fig. 7. Table 4 further illustrates the effective mass for each global vibration mode between the original model and contrast model.

In order to compare the modal analysis results between the original model with rigid hinge and the contrast model without rigid hinge, three parameters representing the dynamic characteristics of the bridge are used. The first and second parameters are the modal frequency and effective mass of each vibration mode, respectively. The third parameter is the modal assurance criterion (MAC) index which is used to evaluate the correlation of mode shapes between the original model and contrast model. The MAC index is defined as (Ren and Peng 2005)

$$\text{MAC}(\boldsymbol{\varphi}_a, \boldsymbol{\varphi}_e) = \frac{|\boldsymbol{\varphi}_a^T \boldsymbol{\varphi}_e|^2}{(\boldsymbol{\varphi}_a^T \boldsymbol{\varphi}_a)(\boldsymbol{\varphi}_e^T \boldsymbol{\varphi}_e)} \quad (1)$$

where  $\phi_a$  and  $\phi_e$  are the mode shapes obtained from the original model and contrast model, respectively. It should be noted that the comparisons of modal participation factor are similar to the effective mass and hence the comparison results of modal participation factor are not listed.

Comparing the modal analysis results between the original model with rigid hinge and the contrast model without rigid hinge, it can be seen that:

(i) The modal frequency of the first symmetric lateral bending mode of bridge deck of the contrast model is 0.8610 Hz, while the modal frequency of the original model is 0.7087 Hz with the mode order 21. The relative variation is about 21.50%. Fig. 8(a) further shows the comparison of the mode shapes with regard to the original model and contrast model. The value of MAC is 0.9998, which indicates a good correlation between the mode shapes with and without rigid hinge. Hence, the installation of rigid hinge significantly reduces the modal frequency of the first symmetric lateral bending mode of bridge deck, but it has a limited effect on changing the mode shape of the vibration mode.

(ii) The modal frequency of the first symmetric torsional mode of bridge deck of the contrast model is 1.1386 Hz, while the modal frequency of the original model is 1.1361 Hz with the mode order 43. The relative variation is only about 0.22%. However, the mode shape of the bridge deck of the contrast model is very different from that of the original model. As shown in Fig. 6(f), the torsional mode of the original model with rigid hinge only occurs in one span in the middle of the bridge deck. However, the torsional mode of the contrast model without rigid hinge occurs in three

Table 3 Influence of rigid hinge on the dynamic characteristics of the bridge

Modal frequency /Hz		Description of vibration modes
Original model with rigid hinge	Contrast model without rigid hinge	
0.2274	0.2299	1st symmetric vertical bending of bridge deck+ symmetric longitudinal bending of bridge tower
0.2615	0.2615	1st anti-symmetric vertical bending of bridge deck+ anti-symmetric longitudinal bending of bridge tower
0.2894	0.2894	1st symmetric lateral bending of bridge tower
0.2907	0.2907	1st anti-symmetric lateral bending of bridge tower
0.2928	0.2928	2nd symmetric lateral bending of bridge tower
0.2950	0.2950	2nd anti-symmetric lateral bending of bridge tower
0.2965	0.2965	3rd symmetric lateral bending of bridge tower
0.2970	0.2970	3rd anti-symmetric lateral bending of bridge tower
0.3085	0.3089	2nd symmetric vertical bending of bridge deck+ symmetric longitudinal bending of bridge tower
0.3618	0.3618	2nd anti-symmetric vertical bending of bridge deck+ anti-symmetric longitudinal bending of bridge tower
0.6779	0.6779	Longitudinal bending of bridge piers
0.7087	0.8610	1st symmetric lateral bending of bridge deck+ symmetric lateral bending of bridge tower
0.8956	0.8956	1st anti-symmetric lateral bending of bridge deck+ anti-symmetric lateral bending of bridge tower
1.1361	1.1386	1st symmetric torsion of bridge deck
1.1389	1.1389	2nd symmetric torsion of bridge deck
1.1391	1.1392	3rd symmetric torsion of bridge deck

spans in the middle of the bridge deck as shown in Fig. 7(f). For clear representation, the normalized mode shapes of the first symmetric torsional mode of bridge deck are further shown in Fig. 8(b). The value of MAC is 0.6619, which indicates a poor correlation between the mode shapes with and without rigid hinge. And from Table 4, it can be seen that the effective mass of the first symmetric torsional mode of bridge deck of the contrast model is far less than that of the original model, which means that the contribution of the first symmetric torsional mode of bridge deck increases with the installation of the rigid hinge. Considering the significance of the torsional mode on the wind-resistance performance of the long-span bridge, the changes of the mode shape and effective mass of the first symmetric torsional mode of bridge deck due to the rigid hinge deserves special attention.

(iii) Except for the first symmetric lateral bending mode of bridge deck and the first symmetric torsional mode of bridge deck, the rigid hinge in the middle of the main girder has a limited effect on changing the modal frequencies, mode shapes and effective masses of other global vibration modes.

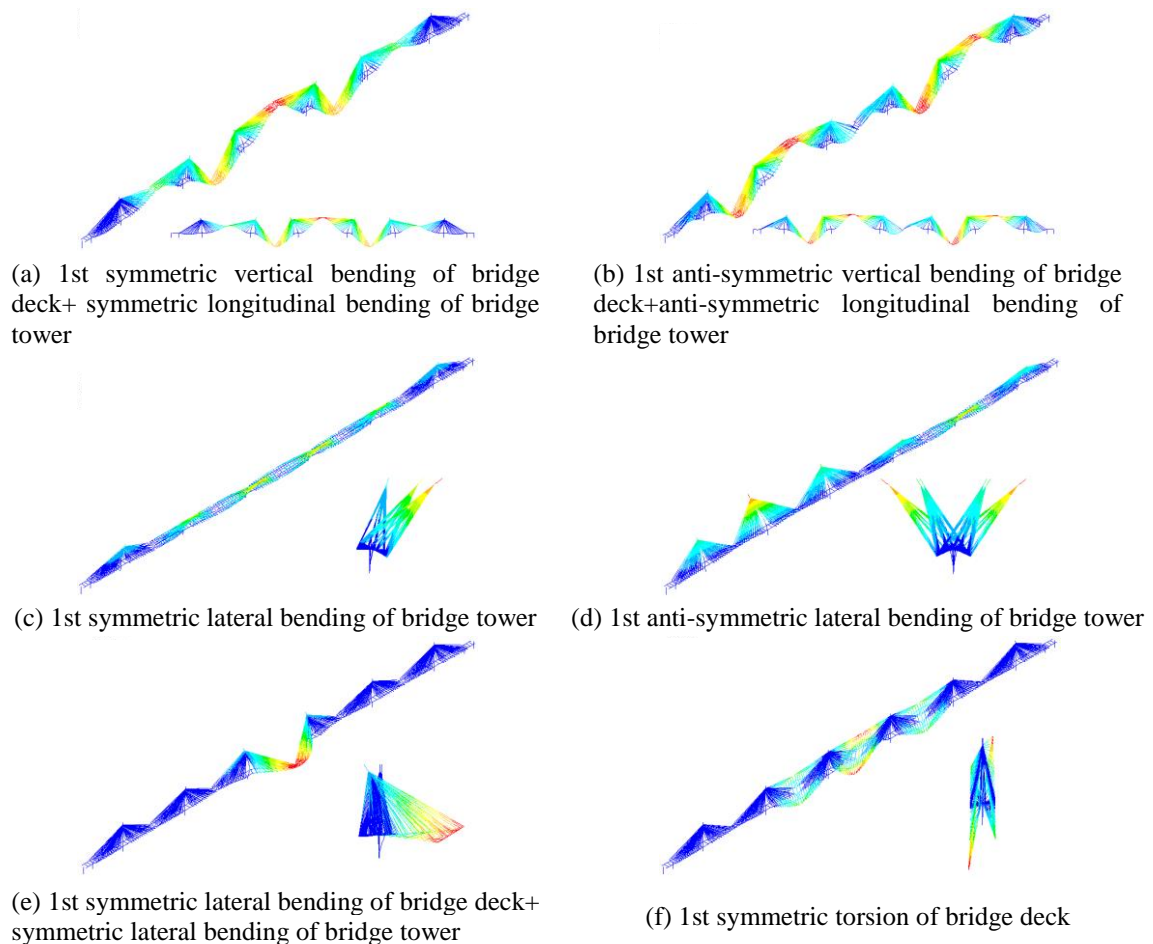
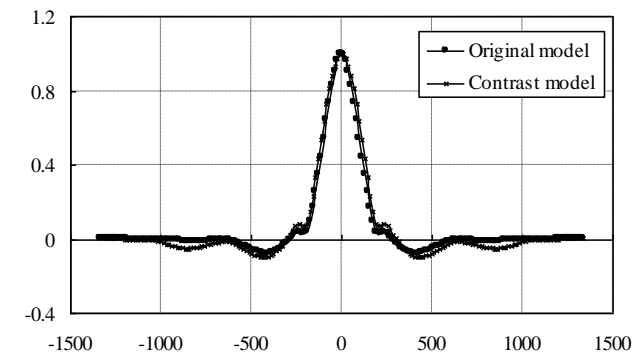


Fig. 7 Mode shapes of the contrast model without rigid hinge

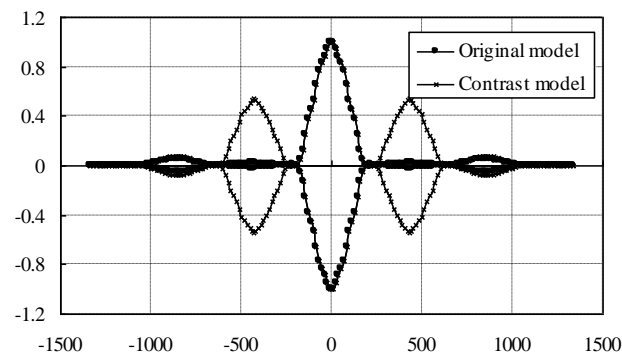
Table 4 Comparisons of effective mass for each global vibration mode

Mode No.*	X direction (Longitudinal direction)		Y direction (Vertical direction)		Z direction (Transverse direction)	
	Original model	Contrast model	Original model	Contrast model	Original model	Contrast model
1	-8.720E-01	-7.310E-06	<b>2.974E+02</b>	<b>2.847E+02</b>	-2.640E-06	-1.240E-06
2	<b>-1.247E+03</b>	<b>-1.247E+03</b>	8.180E-02	4.750E-06	-1.130E-05	-5.970E-07
3	-7.300E-07	2.270E-07	1.840E-06	-3.780E-07	<b>9.857E+03</b>	<b>9.860E+03</b>
4	-5.560E-07	7.950E-08	-1.720E-06	1.580E-07	5.610E-02	1.270E-05
5	-7.380E-07	-1.770E-07	1.230E-06	-6.840E-07	<b>3.395E+03</b>	<b>3.385E+03</b>
6	-1.070E-06	2.470E-07	8.550E-07	-1.200E-07	-4.490E-02	-1.710E-06
7	1.390E-07	6.670E-08	5.510E-07	-1.010E-07	<b>2.870E+03</b>	<b>2.864E+03</b>
8	6.610E-08	-2.930E-08	4.360E-07	5.070E-08	3.800E-02	2.380E-05
9	4.020E-01	3.880E-06	<b>-1.017E+03</b>	<b>9.854E+02</b>	9.300E-06	1.700E-06
10	<b>9.717E+02</b>	<b>9.717E+02</b>	-7.720E-02	-6.340E-06	-2.170E-06	-5.720E-07
21	3.870E-07	4.982E+02	2.520E-08	1.430E-11	<b>3.285E+03</b>	<b>3.474E+03</b>
33	-8.920E-08	2.990E-07	-4.050E-06	-2.590E-06	1.675E-01	1.510E-07
43	1.090E-06	1.770E-07	-5.230E-07	6.900E-06	<b>-5.328E+02</b>	<b>-6.129E+01</b>
44	-2.130E-05	-4.840E-06	2.190E-06	6.870E-07	2.170E-03	2.290E-05
45	-2.710E-06	-8.190E-06	-1.990E-06	8.950E-08	<b>-9.264E+01</b>	<b>6.514E+01</b>

\*Note: Here the mode No. is referenced by the modes of the original model.



(a) The first symmetric lateral bending mode of bridge deck



(b) The first symmetric torsional mode of bridge deck

Fig. 8 Comparisons of the mode shapes of the original model and contrast model

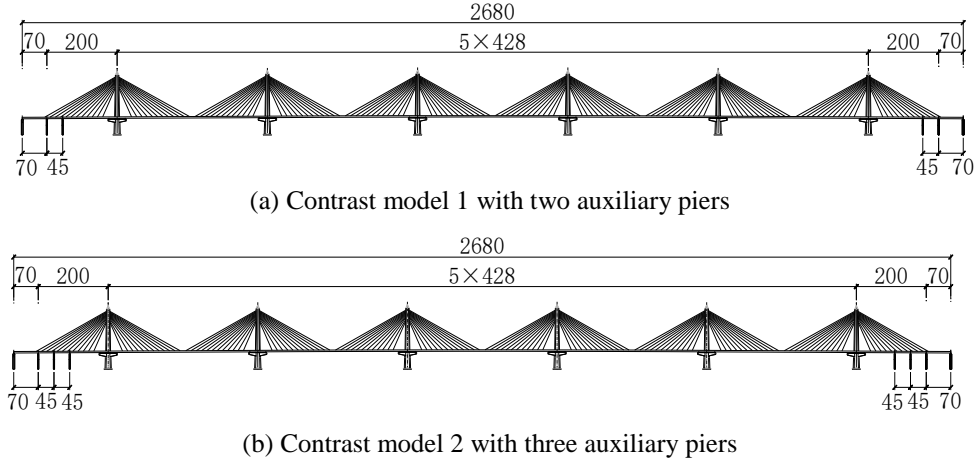


Fig. 9 Arrangement of auxiliary piers in the contrast models (Unit: m)

## 5. Influence of auxiliary pier on the dynamic characteristics

The role of auxiliary piers installed on the side-spans of the multi-span cable-stayed bridge is to increase the structural system stiffness under live loadings because the deflection of the girder in the side-spans can be reduced and then the structural static responses such as internal force and deformation of the bridge tower can also be reduced due to the interaction between the girder and tower. In the design of Mezcala Bridge in Mexico and Sepoong Bridge in Korea, the auxiliary piers are both used for multi-span cable-stayed bridges.

In the present study, in order to investigate the effect of auxiliary piers on the dynamic characteristics of the multi-span cable-stayed bridge, two contrast analytical models are developed based on the original finite element model of Jiashao Bridge: (i) Contrast model 1 with two auxiliary piers installed in each side-span; (ii) Contrast model 2 with three auxiliary piers installed in each side-span. The arrangement of auxiliary piers in the contrast models are shown in Fig. 9. The modal analysis results of two contrast models are shown in Table 3. It should be noted that the comparison results indicate that the layout of the auxiliary piers in the side-spans has little effect on changing the calculated effective mass and modal participation factor for each global vibration mode. Thus, the calculated effective mass and modal participation factor for each global vibration mode of Contrast model 1 and Contrast model 2 are not listed.

Comparing the modal analysis results between the original model and two contrast models shown in Table 5, it can be seen that:

(i) The modal frequencies of vertical and lateral bending modes of bridge deck, lateral bending modes of bridge tower are slightly increased with the increase of auxiliary piers. Compared with the original model, the first symmetric vertical bending mode of bridge deck of Contrast model 1 and Contrast model 2 increases from 0.2274Hz to 0.2280Hz and 0.2281Hz, respectively. The relative variation is about 0.26% and 0.31%, respectively. The first symmetric lateral bending mode of bridge deck increases from 0.7087Hz to 0.7088Hz and 0.7089Hz, respectively. The relative variation is about 0.01% and 0.03%, respectively. Fig. 10(a) and Fig. 10(b) further show the comparisons of the first symmetric vertical bending mode and the first symmetric lateral bending mode of bridge deck with regard to the original model and contrast model 2. The values

of MAC for the first symmetric vertical bending mode and the first symmetric lateral bending mode of bridge deck are 0.9962 and 0.9999, respectively, which indicates that the auxiliary piers have little effect on changing the mode shapes of vertical and lateral bending modes of bridge deck except for two-end side-spans.

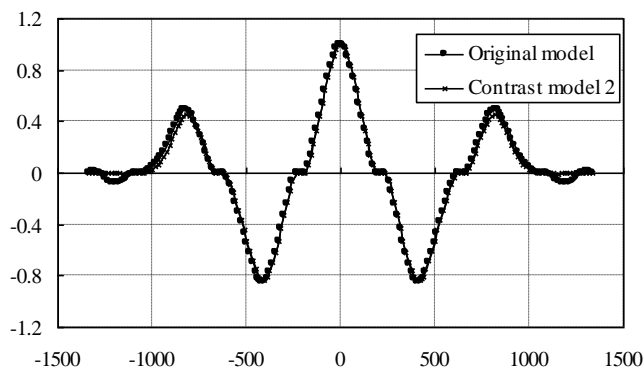
(ii) The modal frequencies of torsional modes of bridge deck are decreased a little with the increase of auxiliary piers. Compared with the original model, the first torsional mode of bridge deck of Contrast model 1 and Contrast model 2 decreases from 1.1361Hz to 1.1307Hz and 1.1278Hz, respectively. The relative variation is only about 0.48% and 0.73%, respectively. Fig. 10(c) further shows the comparison of the first torsional mode of bridge deck with regard to the original model and contrast model 2. The values of MAC for the first torsional mode of bridge deck is 0.9999, which indicates that the auxiliary piers have little effect on changing the mode shapes of torsional modes of bridge deck.

(iii) The number of the longitudinal bending modes of auxiliary piers increases correspondingly with the increase of auxiliary piers. However, the frequencies of these local vibration modes are all the same with 0.6779Hz for original model and two contrast models.

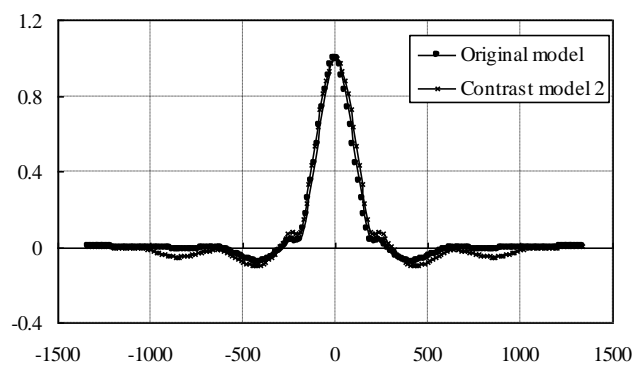
On the whole, the layout of the auxiliary piers in the side-spans has a limited effect on changing the modal frequencies, mode shapes and effective masses of global vibration modes.

Table 5 Influence of auxiliary pier on the dynamic characteristics of the bridge

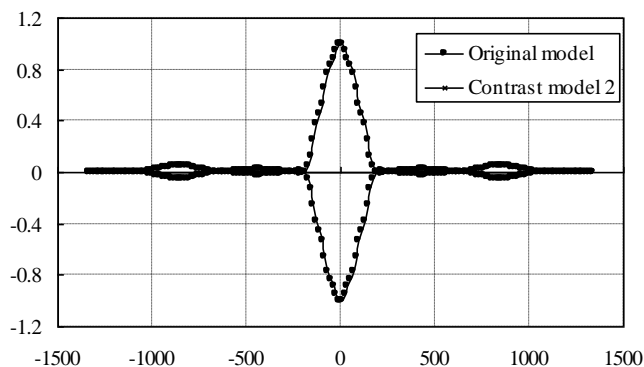
Modal frequency /Hz			Description of vibration modes
Original model	Contrast model 1	Contrast model 2	
0.2274	0.2280	0.2281	1st symmetric vertical bending of bridge deck + symmetric longitudinal bending of bridge tower
0.2615	0.2641	0.2645	1st anti-symmetric vertical bending of bridge deck + anti-symmetric longitudinal bending of bridge tower
0.2894	0.2895	0.2895	1st symmetric lateral bending of bridge tower
0.2907	0.2910	0.2911	1st anti-symmetric lateral bending of bridge tower
0.2928	0.2932	0.2934	2nd symmetric lateral bending of bridge tower
0.2950	0.2956	0.2957	2nd anti-symmetric lateral bending of bridge tower
0.2965	0.2985	0.3003	3rd symmetric lateral bending of bridge tower
0.2970	0.2986	0.3003	3rd anti-symmetric lateral bending of bridge tower
0.3085	0.3133	0.3142	2nd symmetric vertical bending of bridge deck + symmetric longitudinal bending of bridge tower
0.3618	0.3690	0.3702	2nd anti-symmetric vertical bending of bridge deck + anti-symmetric longitudinal bending of bridge tower
0.6779	0.6779	0.6779	Longitudinal bending of bridge piers
0.7087	0.7088	0.7089	1st symmetric lateral bending of bridge deck + symmetric lateral bending of bridge tower
0.8956	0.8958	0.8960	1st anti-symmetric lateral bending of bridge deck + anti-symmetric lateral bending of bridge tower
1.1361	1.1307	1.1278	1st symmetric torsion of bridge deck
1.1389	1.1333	1.1303	2nd symmetric torsion of bridge deck
1.1391	1.1334	1.1305	3rd symmetric torsion of bridge deck



(a) The first symmetric vertical bending mode of bridge deck



(b) The first symmetric lateral bending mode of bridge deck



(c) The first symmetric torsional mode of bridge deck

Fig. 10 Comparisons of the mode shapes of the original model and contrast model 2

## 6. Influence of longitudinal constraint on the dynamic characteristics

In the structural design of Jiashao Bridge, the longitudinal constraints between the girders and side tower No. 2, the girders and side tower No. 5 are employed, respectively. The role of such partially constrained system is to restrain the temperature-induced longitudinal deformation of the

bridge girders. In order to investigate the effect of longitudinal constraint on the dynamic characteristics of the multi-span cable-stayed bridge, two contrast analytical models are developed based on the original finite element model of Jiashao Bridge: (i) Contrast model 1: the longitudinal constraints between the girders and all six towers are employed in the bridge, i.e., fully constrained system; (ii) Contrast model 2: the longitudinal constraints between the girders and all six towers are released in the bridge, i.e., fully floating system. The modal analysis results of two contrast models are shown in Table 6 and Table 7, respectively. Table 8 further illustrates the effective mass for each global vibration mode.

Table 6 Vibration modes of contrast model 1 with fully constrained system

Mode No.	Modal frequency /Hz	Description
1	0.2376	1st symmetric vertical bending of bridge deck + symmetric longitudinal bending of bridge tower
2	0.2694	1st anti-symmetric vertical bending of bridge deck + anti-symmetric longitudinal bending of bridge tower
3	0.2895	1st symmetric lateral bending of bridge tower
4	0.2910	1st anti-symmetric lateral bending of bridge tower
5	0.2931	2nd symmetric lateral bending of bridge tower
6	0.2952	2nd anti-symmetric lateral bending of bridge tower
7	0.2968	3rd symmetric lateral bending of bridge tower
8	0.2972	3rd anti-symmetric lateral bending of bridge tower
9	0.3115	2nd symmetric vertical bending of bridge deck + symmetric longitudinal bending of bridge tower
10	0.3630	2nd anti-symmetric vertical bending of bridge deck + anti-symmetric longitudinal bending of bridge tower
16~19	0.6779	Longitudinal bending of bridge piers
28	0.8598	1st symmetric lateral bending of bridge deck + symmetric lateral bending of bridge tower
33	0.9524	1st anti-symmetric lateral bending of bridge deck + anti-symmetric lateral bending of bridge tower
43	1.1366	1st symmetric torsion of bridge deck
44	1.1397	2nd symmetric torsion of bridge deck
45	1.1398	3rd symmetric torsion of bridge deck

Table 7 Vibration modes of contrast model 2 with fully floating system

Mode No.	Modal frequency /Hz	Description
1	0.1704	1st symmetric vertical bending of bridge deck + symmetric longitudinal bending of bridge tower
2	0.1725	Longitudinal floating + 1st anti-symmetric vertical bending of bridge deck + anti-symmetric longitudinal bending of bridge tower
3	0.2304	2nd symmetric vertical bending of bridge deck + symmetric longitudinal bending of bridge tower
4	0.2617	2nd anti-symmetric vertical bending of bridge deck + anti-symmetric longitudinal bending of bridge tower

Table 7 Continued

5	0.2894	1st symmetric lateral bending of bridge tower
6	0.2907	1st anti-symmetric lateral bending of bridge tower
7	0.2927	2nd symmetric lateral bending of bridge tower
8	0.2948	2nd anti-symmetric lateral bending of bridge tower
9	0.2964	3rd symmetric lateral bending of bridge tower
10	0.2969	3rd anti-symmetric lateral bending of bridge tower
18~21	0.6779	Longitudinal bending of bridge piers
23	0.7071	1st symmetric lateral bending of bridge deck + symmetric lateral bending of bridge tower
31	0.8558	1st anti-symmetric lateral bending of bridge deck + anti-symmetric lateral bending of bridge tower
43	1.1357	1st symmetric torsion of bridge deck
44	1.1384	2nd symmetric torsion of bridge deck
45	1.1387	3rd symmetric torsion of bridge deck

Table 8 Comparisons of effective mass for each global vibration mode

Mode No.*	X direction (Longitudinal direction)			Y direction (Vertical direction)			Z direction (Transverse direction)		
	Original model	contrast model 1	contrast model 2	Original model	contrast model 1	contrast model 2	Original model	contrast model 1	contrast model 2
1	-8.720E-01	3.730E-06	2.280E-04	<b>2.974E+02</b>	<b>0.22170E+02</b>	<b>0.22234E+02</b>	-2.640E-06	-4.380E-06	-6.740E-07
2	<b>-1.247E+03</b>	<b>-2.068E+02</b>	<b>1.428E+04</b>	8.180E-02	-1.460E-05	-3.420E-06	-1.130E-05	-1.960E-06	-1.420E-07
3	-7.300E-07	7.500E-07	4.190E-07	1.840E-06	2.160E-06	3.230E-07	<b>9.857E+03</b>	<b>0.39.805E+03</b>	<b>0.39.787E+03</b>
4	-5.560E-07	1.190E-07	1.090E-07	-1.720E-06	1.740E-07	-3.890E-07	5.610E-02	2.960E-05	3.970E-06
5	-7.380E-07	3.700E-07	2.450E-07	1.230E-06	1.680E-06	-7.370E-07	<b>3.395E+03</b>	<b>0.33.560E+03</b>	<b>0.33.597E+03</b>
6	-1.070E-06	5.350E-07	-2.410E-07	8.550E-07	1.190E-06	-3.750E-07	-4.490E-02	3.950E-06	-2.640E-06
7	1.390E-07	1.240E-07	-2.220E-07	5.510E-07	7.830E-07	4.370E-07	<b>2.870E+03</b>	<b>0.32.819E+03</b>	<b>0.32.882E+03</b>
8	6.610E-08	-1.090E-07	2.510E-07	4.360E-07	5.540E-07	7.830E-08	3.800E-02	1.340E-05	8.420E-06
9	4.020E-01	-8.620E-06	-5.340E-06	<b>-1.017E+03</b>	<b>1.083E+03</b>	<b>9.579E+02</b>	9.300E-06	-1.720E-05	-4.190E-06
10	<b>9.717E+02</b>	<b>0.29.234E+02</b>	<b>0.25.322E+02</b>	-7.720E-02	1.030E-05	2.070E-06	-2.170E-06	1.360E-07	1.930E-06
21	3.870E-07	8.298E-08	-1.140E-07	2.520E-08	-2.530E-07	-2.620E-06	<b>3.285E+03</b>	<b>0.36.844E+03</b>	<b>0.33.100E+03</b>
33	-8.920E-08	5.980E-06	8.080E-07	-4.050E-06	3.060E-06	-1.140E-08	1.675E-01	-1.510E-06	1.320E-06
43	1.090E-06	-3.250E-06	4.380E-07	-5.230E-07	2.240E-06	1.450E-06	<b>-5.328E+02</b>	<b>-2.562E+02</b>	<b>-5.857E+02</b>
44	-2.130E-05	3.860E-06	-5.180E-06	2.190E-06	1.630E-06	2.060E-06	2.170E-03	5.270E-05	-3.600E-06
45	-2.710E-06	3.580E-07	-4.260E-06	-1.990E-06	-1.170E-06	6.510E-07	<b>-9.264E+01</b>	<b>-5.232E+01</b>	<b>1.707E+01</b>

\*Note: Here the mode No. is referenced by the modes of the original model.

Comparing the modal analysis results between the original model and two contrast models, it can be seen that:

(i) The longitudinal floating vibration mode occurs in the contrast model 2 with fully floating system. But in the original model with partially constrained system and contrast model 1 with fully

constrained system, the longitudinal floating vibration mode doesn't occur due to the longitudinal constraints between the bridge girders and towers. From Table 8, it can be seen that the effective mass of the vibration mode No.2 in the longitudinal direction of the contrast model 2 is significantly larger than that of the original model and contrast model 1.

(ii) The modal frequency of the first symmetric vertical bending mode of bridge deck of the contrast model 1 with fully constrained system is 0.2376Hz, while the modal frequency of the contrast model 2 with fully floating system is 0.1704Hz. The relative variation is about 28.29%. And the modal frequencies of the first anti-symmetric vertical bending of bridge deck of the contrast model 1 and contrast model 2 are 0.2694Hz and 0.1725Hz, respectively. The relative variation is about 35.97%. Hence, the application of the longitudinal constraints between the bridge girders and towers significantly increase the modal frequencies of the vertical bending modes of the bridge deck. Fig. 11(a) and Fig. 11(b) further show the comparisons of the vertical bending modes of bridge deck with regard to the original model and contrast model 1. The corresponding values of MAC are 0.9997 and 0.9996, respectively. Hence, the model shape of contrast model 1 with fully constrained system is almost the same as that of original model with partially constrained system. Fig. 12(a) and Fig. 12(b) show the comparisons of the vertical bending modes of bridge deck with regard to the original model and contrast model 2. The corresponding values of MAC are 0.5077 and 0.0240, which indicates that the model shape of contrast model 2 with fully floating system is very different from that of original model with partially constrained system.

(iii) The modal frequency of the first symmetric lateral bending mode of bridge deck of the contrast model 1 with fully constrained system is 0.8598Hz, while the modal frequency of the contrast model 2 with fully floating system is 0.7071Hz. The relative variation is about 17.76%. And the modal frequencies of the first anti-symmetric lateral bending of bridge deck of the contrast model 1 and contrast model 2 are 0.9524Hz and 0.8558Hz, respectively. The relative variation is about 10.14%. Hence, the application of the longitudinal constraints between the bridge girders and towers significantly increase the modal frequencies of the lateral bending modes of the bridge deck. Fig. 11(c) and Fig. 11(d) further show the comparisons of the lateral bending modes of bridge deck with regard to the original model and contrast model 1. The corresponding values of MAC are 0.8460 and 0.9866. Hence, the model shape of the first symmetric lateral bending mode of bridge deck in the contrast model 1 with fully constrained system is a little different from that of original model with partially constrained system. Fig. 12(c) and Fig. 12(d) show the comparisons of the lateral bending modes of bridge deck with regard to the original model and contrast model 2. The corresponding values of MAC are 0.9965 and 0.0297. Hence, with regard to the first anti-symmetric lateral bending of bridge deck, the model shape of contrast model 2 with fully floating system is very different from that of original model with partially constrained system.

(iv) The modal frequency of the first symmetric lateral bending mode of bridge tower of the contrast model 1 with fully constrained system is 0.2895Hz, while the modal frequency of the contrast model 2 with fully floating system is 0.2894Hz. The relative variation is only about 0.03%, which indicates that the application of the longitudinal constraints has little effect on the modal frequencies of lateral bending modes of bridge tower.

(v) The modal frequency of the first symmetric torsional mode of bridge deck of the contrast model 1 with fully constrained system is 1.1366Hz, while the modal frequency of the contrast model 2 with fully floating system is 1.1357Hz. The relative variation is only about 0.08%, which indicates that the application of the longitudinal constraints has little effect on the modal

frequencies of torsional modes of bridge deck. Fig. 11(e) and Fig. 12(e) show the comparisons of the first symmetric torsional mode of bridge deck. The corresponding values of MAC are 0.9663 and 0.9849, respectively. Hence, the model shape of contrast model 2 with fully floating system is almost the same as that of original model with partially constrained system. However, the torsional mode of the contrast model 1 with fully constrained system occurs in three spans in the middle of the bridge deck, which is a little different from the mode shape of the original model.

On the whole, the application of longitudinal constraints between the bridge girders and towers increases the modal frequencies of the vertical bending modes and lateral bending modes of bridge deck. Moreover, the longitudinal constraints have significant effects on changing the mode shapes

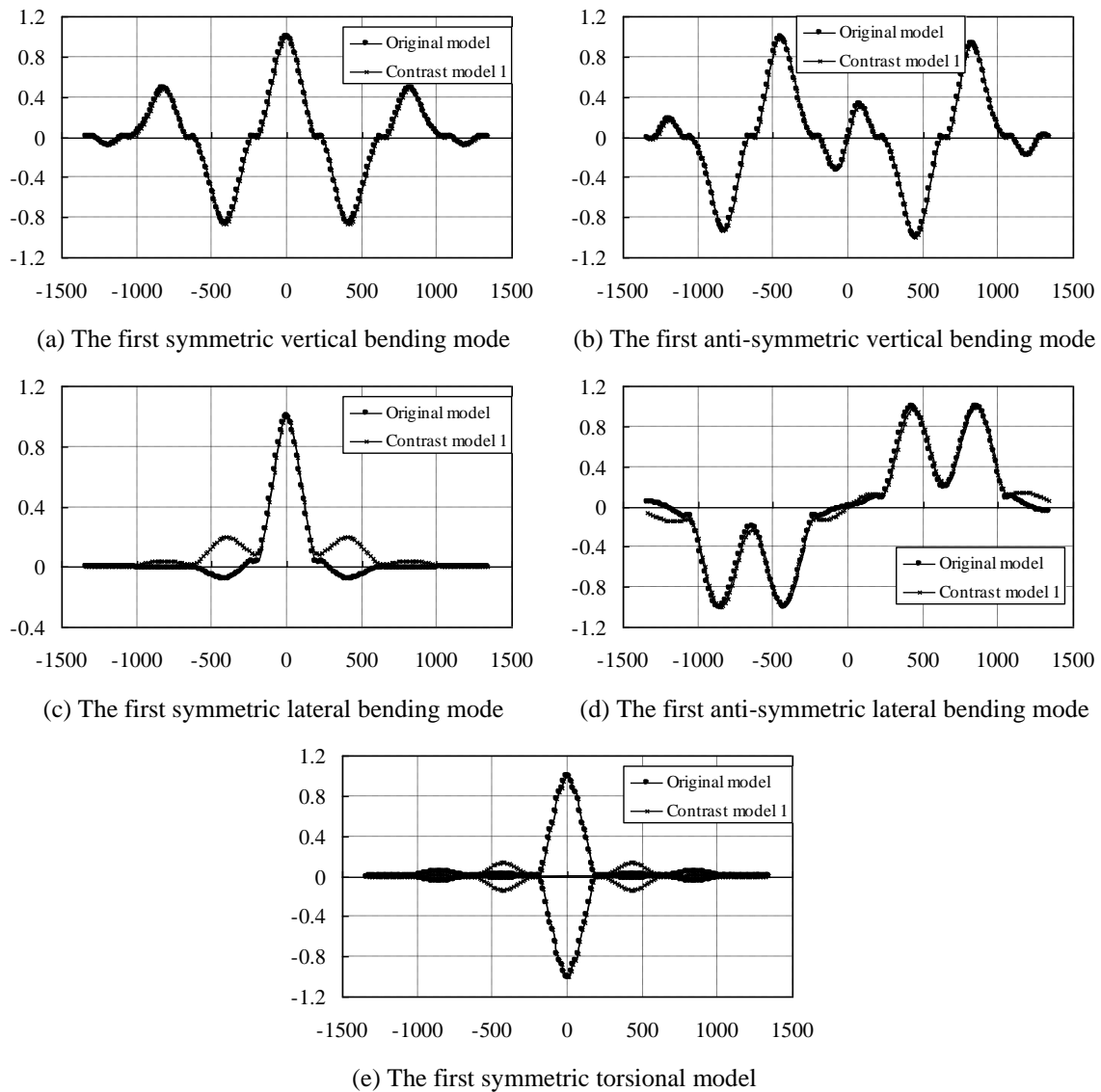


Fig. 11 Comparisons of the mode shapes of the original model and contrast model 1

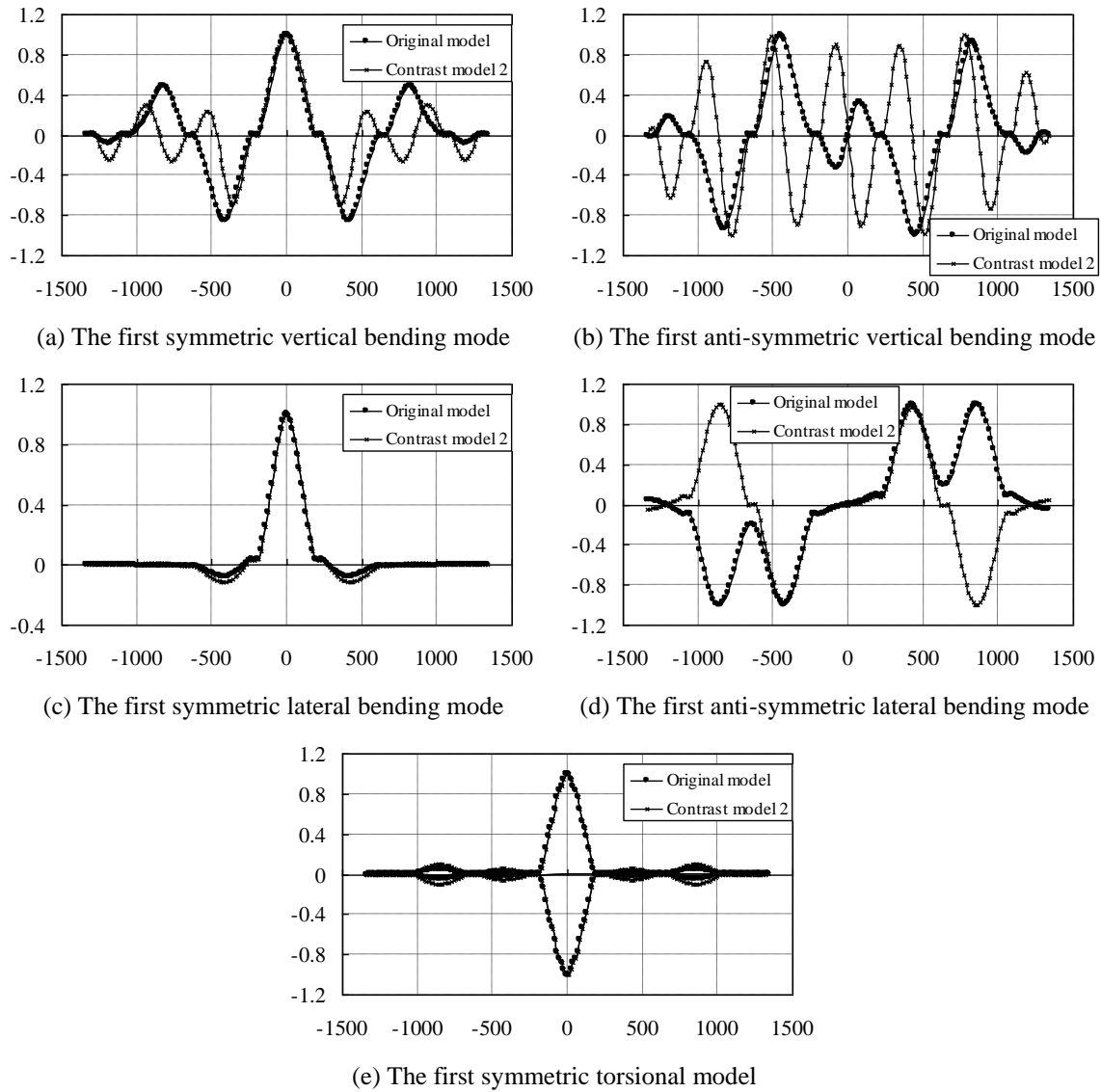


Fig. 12 Comparisons of the mode shapes of the original model and contrast model 2

of vertical bending modes and lateral bending modes of bridge deck and the effective mass of the first anti-symmetric vertical bending of bridge deck in the longitudinal direction of the fully floating system is significantly larger than that of the partially constrained system and fully constrained system, which deserves special attention when conducting seismic analysis and wind-induced vibration analysis. Except for the vertical bending modes and lateral bending modes of bridge deck, the longitudinal constraints have a limited effect on changing the modal frequencies, mode shapes and effective masses of other global vibration modes.

## 7. Conclusions

The Jiaoshao Bridge in China is the longest multi-span cable-stayed bridge in the world. In order to overcome the problems of insufficient system stiffness and large temperature deformation in the long girders, three important structural measures including the rigid hinge, auxiliary piers and longitudinal constraints between the girders and towers are applied in the design of Jiashao Bridge. In this paper, the dynamic properties of the Jiashao Bridge and the influences of these important structural measures on the dynamic properties of the bridge were studied. The following conclusions for this multi-span cable-stayed bridge are obtained.

- For the Jiashao Bridge, the longitudinal floating vibration mode doesn't occur due to the longitudinal constraints between the bridge girders and towers. The first vertical bending mode of bridge deck with a frequency of 0.2274Hz occurs at the 1st global mode, which is lower than the corresponding value 0.7087Hz of the first lateral bending mode. Hence, the in-plane stiffness of bridge deck is weaker than the out-plane stiffness. The natural frequency of the first symmetric lateral bending of bridge tower is found to be 0.2894Hz which is the third global vibration mode. Hence, the bridge towers are flexible with regard to the lateral bending. Meanwhile, the first torsional mode of the bridge deck with a frequency of 1.1361Hz occurs at the 43rd global mode, which indicates that the higher torsional stiffness of the bridge deck is favorable for wind-resistance performance.

- The installation of the rigid hinge significantly reduces the modal frequency of the first symmetric lateral bending mode of bridge deck by about 21.50%, while the rigid hinge has a limited effect on changing the mode shape of the first symmetric lateral bending mode of bridge deck. On the contrary, the installation of the rigid hinge significantly changes the mode shape and effective mass of the first symmetric torsional mode of bridge deck, while the relative variation of the modal frequency of this vibration mode is only about 0.22%. Except for the first symmetric lateral bending mode of bridge deck and the first symmetric torsional mode of bridge deck, the rigid hinge in the middle of the main girder has a limited effect on changing the modal frequencies, mode shapes and effective masses of other global vibration modes.

- The modal frequencies of vertical and lateral bending modes of bridge deck, lateral bending modes of bridge tower are slightly increased with the increase of auxiliary piers. On the contrary, the modal frequencies of torsional modes of bridge deck are decreased a little with the increase of auxiliary piers. On the whole, the layout of the auxiliary piers in the side-spans has a limited effect on changing the modal frequencies, mode shapes and effective masses of global vibration modes.

- With regard to the longitudinal constraints between the bridge girders and towers, the employment of the longitudinal constraints significantly increases the modal frequencies of the vertical bending modes and lateral bending modes of bridge deck. Moreover, the longitudinal constraints have significant effects on changing the mode shapes of vertical bending modes and lateral bending modes of bridge deck. And the effective mass of the first anti-symmetric vertical bending of bridge deck in the longitudinal direction of the fully floating system is significantly larger than that of the partially constrained system and fully constrained system. Except for the vertical bending modes and lateral bending modes of bridge deck, the longitudinal constraints have a limited effect on changing the modal frequencies, mode shapes and effective masses of other global vibration modes including the lateral bending modes of the bridge towers and torsional modes of the bridge deck.

## Acknowledgments

The research described in this paper was financially supported by the National Science and Technology Support Program (No. 2014BAG07B01), National Natural Science Foundation of China (No. 51178100) and Key Program of Ministry of Transport (No. 2011318223170 & No. 2013319223120).

## References

- Barre, C., Flamand, O. and Grillaud, G. (1999), "The Millau viaduct - a special wind studies for an exceptional structure", *Proceedings of the 10th International Conference on Wind Engineering*, Copenhagen, Denmark, August.
- Ding, Y.L., Li, A.Q., Sun, J. and Deng, Y. (2008), "Experimental and analytical studies on static and dynamic characteristics of steel box girder for Runyang Cable-stayed Bridge", *Adv. Struct. Eng.*, **11**(4), 425-438.
- He, G.J., Zou, Z.Q., Ni, Y.Q. and Ko, J.M. (2009), "Seismic response analysis of multi-span cable-stayed bridge", *Proceedings of the 2nd International Conference on Advances in Concrete and Structures*, Changsha, China, July.
- Li, H., Laima, S.J., Li, N., Ou, J.P. and Duan, Z.D. (2010), "Correlation analysis of the wind of a cable-stayed bridge based on field monitoring", *Wind Struct.*, **13**(6), 529-556.
- Li, H., Liu, J.L. and Ou, J.P. (2009), "Investigation of seismic damage of cable-stayed bridges with different connection configuration", *J. Earthq. Tsunami*, **3**(3), 227-247.
- Li, Z.X., Zhou, T.Q., Chan, T.H.T. and Yu, Y. (2007), "Multi-scale numerical analysis on dynamic response and local damage in long-span bridges", *Eng. Struct.*, **29**(7), 1507-1524.
- Ni, Y.Q., Wang, J.Y. and Lo, L.C. (2005), "Influence of stabilizing cables on seismic response of a multispan cable-stayed bridge", *Comput. Aid. Civil Infrast. Eng.*, **20**(2), 142-153.
- Papanikolas, P. (2003), "The Rion-Antirion multispan cable-stayed bridge", *Proceedings of the 2nd MIT Conference on Computational Fluid and Solid Mechanics*, Cambridge, MA, June.
- Raheem, S.E.A., Hayashikawa, T. and Dorka, U. (2011), "Ground motion spatial variability effects on seismic response control of cable-stayed bridges", *Earthq. Eng. Eng. Vib.*, **10**(1), 37-49.
- Ren, W.X. and Peng, X.L. (2005), "Baseline finite element modeling of a large span cable-stayed bridge through field ambient vibration tests", *Comput. Struct.*, **83**(8-9), 536-550.
- Ren, W.X., Lin, Y.Q. and Peng, X.L. (2007), "Field load tests and numerical analysis on Qingzhou cable-stayed Bridge", *J. Bridge Eng.*, ASCE, **12**(2), 261-270.
- Su, C., Han, D.J., Yan, Q.S. *et al.* (2003), "Wind-induced vibration analysis of the Hong Kong Ting Kau Bridge", *Proceedings of the Institution of Civil Engineers- Structures and Buildings*, **156**(3), 263-272.
- Virlogeux, M. (1999), "Recent evolution of cable-stayed bridges", *Eng. Struct.*, **21**(8), 737-755.
- Wang, H., Zou, K.G., Li, A.Q. and Jiao, C.K. (2010), "Parameter effects on the dynamic characteristics of a super-long-span triple-tower suspension bridge", *J. Zhejiang Univ.-Sci. A*, **11**(5), 305-316.
- Zhang, Q.W., Chang, T.Y.P. and Chang, C.C. (2001), "Finite-element model updating for the Kap Shui Mun cable-stayed bridge", *J. Bridge Eng.*, ASCE, **6**(4), 285-294.